

3D numerical modeling of longwall mining with top-coal caving

N.E. Yasitli, B. Unver*

Department of Mining Engineering, Hacettepe University, Beytepe 06532, Ankara, Turkey

Accepted 8 August 2004

Available online 23 December 2004

Abstract

There is a considerable amount of lignite reserve in the form of thick seams in Turkey. It is rather complicated to predict the characteristics of strata response to mining operation in thick seams. However, a comprehensive evaluation of ground behavior is a prerequisite for maintaining efficient production, especially when the top-coal-caving method behind the face is applied. Top-coal caving is the key factor affecting the efficiency of production at thick-coal seams. During production of top coal by caving behind the face not only a significant amount of coal is lost in the goaf but the coal drawn by means of caving is diluted considerably with surrounding rock. Therefore, it is not possible to carry out an efficient production operation unless caving of top coal behind the face is optimized. In this paper, results of 3D modeling of the top-coal-caving mechanism by using the finite difference code FLAC^{3D} at the M3 longwall panel of the Omerler Underground Mine located at Tuncbilek (Turkey) are presented. According to the modeling results, maximum vertical abutment stresses were formed at a distance of 7 m in front of the face. An analysis of the conditions of top coal has revealed that a 1.5 m thick layer of coal just above the shield supports is well fractured. However, a 3.5 m thick layer of coal above the fractured part is either not fractured or is fractured in the form of large blocks leading to obstruction of windows of shields during coal drawing. It is concluded that, in order to decrease dilution and increase extraction ratio and efficiency of operation, top coal should be as uniformly fractured as possible. Hence, an efficient and continuous coal flowing behind the face can be maintained. A special pre-fracture blasting strategy just sufficient enough to form cracks in the top coal is suggested by means of comparing with the results of numerical modeling.

© 2004 Elsevier Ltd. All rights reserved.

1. Introduction

Coal seams may be classified as thick, moderate and thin. Thick-coal seam categorization differs among countries, but a thickness of 4.8 m is accepted as the lower limit [1]. Thick seams comprise half of the world's coal reserve and 70–80% of thick-coal seams are produced by means of underground mining methods [2,3]. Production methods at the former Yugoslavia, Hungary, Poland, France, India and China are generally similar; however, differences arise due to local conditions [4–8].

Thick-coal-seam mining is different from conventional single-slice coal mining in many aspects.

Although there are operating longwall faces up to a height of 6 m in some parts of the world, in practice it is difficult to extract a slice of more than 4 m. Depending on the local characteristics of a coal seam, such as seam, inclination, continuity, surrounding rock and coal seam mechanical properties and susceptibility of coal to spontaneous combustion, a face height of 2–2.5 m is preferred.

Production of thick seams having variable slope and thickness may prevent the application of slicing, hence, a face is located at the floor of the seam and the coal above the face is won by means of caving behind the face [7,8]. Production of thick seams by using top-coal caving is much simpler in comparison to slice mining and requires less development; consequently, the efficiency of production is significantly higher. The top-coal-caving method was first applied in the 1940s in Russia and then subsequently used in France, former

*Corresponding author. Tel.: +90 312 2977 600; fax: +90 312 2992 155.

E-mail address: unver@hacettepe.edu.tr (B. Unver).

Yugoslavia, Hungary, Romania, former Czechoslovakia and Turkey. The method has been in use in China and India since the 1980s [7,9,10]. At present the method is used extensively in China and India. There are a couple of mines using the method in former Yugoslavia and Turkey, whereas in other countries due to depletion of reserves, geological constraints, technological and economical reasons the method is not used at present. Although this method is not currently used extensively in France and former Yugoslavia, these countries had conducted pioneering work for other countries for the development of the production method.

Despite being an attractive method due to higher production efficiency and lower development requirements, longwall mining with the top-coal-caving method imposed significant difficulties in terms of flowing characteristics of coal, timing and rate of coal drawing, loss of coal in the goaf and dilution. The primary purpose of this research was to investigate the above-stated shortcomings and find ways to overcome difficulties related mainly to top-coal caving.

There have been numerous efforts to improve the efficiency of thick-coal-seam mining. Jha and Karmakar [11] investigated the factors affecting production. Strata behavior during caving and dilution of caved top coal was investigated at in situ conditions by Singh et al. [12]. Singh [1] and Singh et al. [12] determined the formation and behavior of the immediate roof on physical models in the laboratory. Dian [13] made a comparison between slice mining and top-coal-caving methods. Wu [14] tried to determine factors affecting the dilution of coal. Three researchers were mainly focused on the isolation of factors and understanding the phenomenon by means of in situ measurements and observations and constructing physical models. In this study, a numerical model of the M3 longwall panel at the Omerler Underground Mine has been formed in 3D by using commercially available software, FLAC^{3D}. Change of stress distributions has also been determined with the aim of modeling top-coal caving at an operating longwall panel enabling a verification of numerical modeling results with in situ conditions.

2. Omerler underground mine and production method

Omerler Underground Mine is a subsidiary of Turkish Coal Enterprises and is located in the inner Aegean District of Turkey near Tuncbilek–Tavşanlı, Kutahya Province (Fig. 1). It is 13 km from Tavşanlı and 63 km from Kutahya. The total proven lignite reserve in the district is approximately 330 million tonn. The proven reserves suitable for underground and surface production are 263 and 67 million ton,

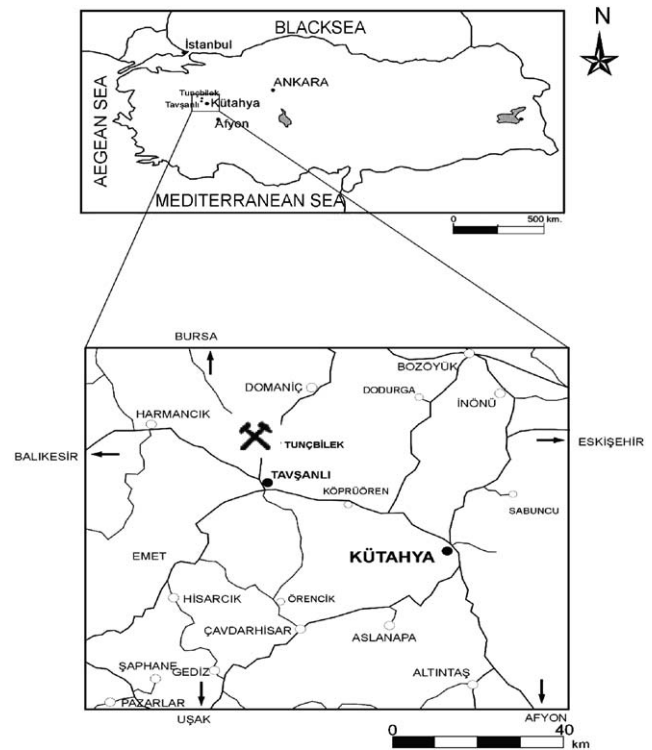


Fig. 1. Location map of GLI region (Tuncbilek).

respectively. The average calorific value of lignite in Tuncbilek District is 4500 kcal/kg, with average sulfur content of 1.5%.

Production started at Omerler Underground Mine in 1985 by retreat longwall with the top-coal-caving method. A conventional support system had been used until 1997, and a fully mechanized face was established in 1997. The average depth below surface is approximately 240 m, and the 8 m thick-coal seam has a slope of 10°.

A generalized stratigraphic column showing the coal seam together with roof and floor strata is presented in Fig. 2. Three main geological units named as claystone, clayey marl and marl are present in the mine area [15]. There is a 30–80 cm thick clay layer 3b at the roof contact of the coal seam frequently creating instability problems due to its low strength and fractured characteristics. There is another claystone layer named as 3a just above the soft clay layer. The claystone 3a layer is stronger than soft clay and its natural moisture content is lower. There is a claystone layer denoted as 3c having an average thickness of 4 m at the floor of the seam. The light gray-colored layer 3c located at the floor is stronger than the dark gray-colored soft claystone 3b and claystone 3a. The coal seam numbered 4 contains three 15, 75 and 55 cm thick clay bands from top to bottom. Physical and mechanical characteristics of coal and surrounding rock are presented in Table 1 [7,15,16,17].

As seen in Fig. 3, six panels were planned for extraction by means of fully mechanized face in sector A. At the time of this study, two adjacent longwall panels, namely M1 and M2, had been completed and the production was carried out at the M3 panel. Coal has been produced by means of longwall retreat with the top-coal-caving production method where a 2.8 m high longwall face was operated at the floor of the coal seam

Thickness	Lithology	Formation
1 m		Top soil
24 m	1	Calcareous marl
189 m	2	Marl
17 m	3a	Claystone
	3b	Soft claystone
8 m	4	Coal
4 m	3 c	Claystone

Fig. 2. A generalized stratigraphic column at Omerler coal mine.

(Fig. 4). Top-slice coal having a thickness of 5.2 m was caved and produced through windows located at the top of the shields.

3. Caving mechanism in the top-coal-caving method

Undoubtedly, caving of naturally fractured or blasted top coal under gravity is the most critical factor in determination of mining method-related parameters such as geometry and dimensions of longwall panel, face support and production scheduling. Top coal usually caves in the form of blocks of various dimensions or small particles and dust. Therefore, a very heterogeneous particle-size distribution is usually present in top coal, leading to complex caving and flowing characteristics. Flowing rules regarding viscous material cannot be applied to fractured solid material. In order to facilitate flowing characteristics, top-coal particle-size distribution should be kept as uniform as possible. The principle of broken solid material flow is independent of size. However, it becomes rather complicated if fine and coarse materials make a heterogeneous mixture. The effect of particle size in the mixture on flowing characteristics is clearly demonstrated in Fig. 5. While a uniform size mixture flows at an angle of 40°, a heterogeneous mixture of fines and blocks will tend to flow at an angle more than 85° from the horizontal plane [18].

3.1. Simple modeling of gravity flow of solid mixture

Caving and drawing of top coal through windows of shields might be simulated with flowing of granulated material in bins and hoppers. Flowing of granulated material in bins and hoppers cannot be considered exactly the same as caving and drawing of coal above the face; however, in terms of the principles of granulated material flow under gravity and coal drawing, a good correlation between the two processes may be established. Gravity flow of blasted coal or roof rock in top-coal caving is a process much more complicated than flow in bins [18,19]. Coarse materials can be very

Table 1
Physical and mechanical properties of coal and surrounding rocks (after Refs. [15,16,7])

Formation	Definition code	Density (MN/m ³)	Porosite (%)	Uniaxial compressive strength (MPa)	Tensile strength (MPa)	Internal friction angle (ϕ)	Cohesion c (MPa)	Modulus of elasticity E (MPa)	Poisson's ratio ν
Calcareous marl	1	0.023	13.8	29.2	3.9	47	12.5	5520	0.26
Marl	2	0.022	—	16.1	1.9	31	5.0	2530	0.25
Roof claystone	3a	0.021	21.30	14.4	2.3	32	3.18	1480	0.28
Soft claystone	3b	0.023	10.8	8.7	1.8	15–35	—	2040	—
Floor claystone	3c	0.024	21.30	26.5	3.5	40	2.90	2085	0.31
Coal	4	0.013	9.72	15.9	—	15–25	—	1733	0.25

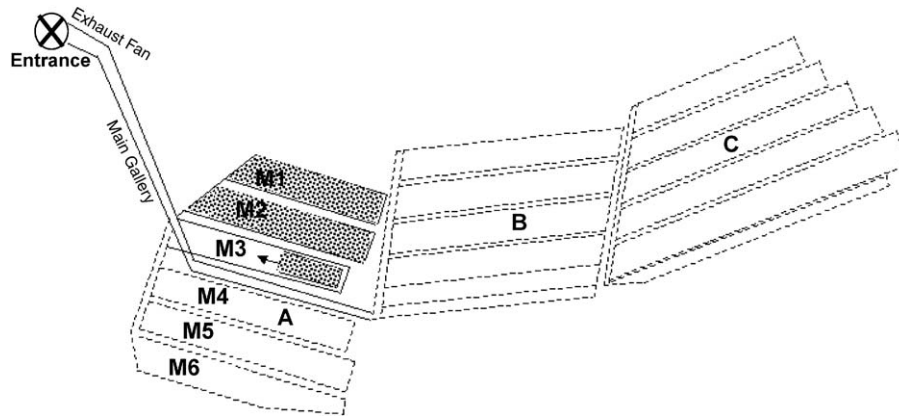


Fig. 3. A simplified plan view of Omerler underground Mine.

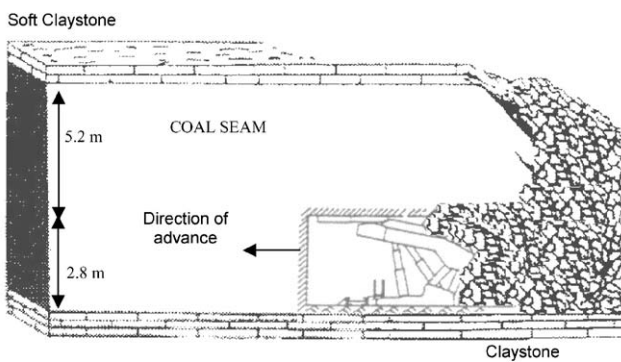


Fig. 4. Longwall with top-coal-caving method as applied at Omerler underground mine.

heterogeneous. Type I shows coarse material with large “spherical” pieces of more or less the same size and shape (Fig. 5). Type II represents a material of almost the same size but different shape. Type III indicates a coarse material composed of large fragments, chippings and small size particles. Type IV represents a coarse material that is characterized as a mixture of large blocks, medium-sized fragments, chippings, sand and/or clay size components. If water is present, in coarse material Type IV, fine particles could create plastic and sticking components. In this case, flowing characteristics of the material would become very unfavorable [18].

Principles of granulated material flow in sublevel or block-caving methods can be considered as similar to the top-coal-caving method. The flowing process is usually demonstrated with a simple vertical glass model with horizontally layered white and black sand filling, as shown in Fig. 6. The glass bin has been designed to observe the motion of sand layers as a consequence of material withdrawal from an opening at the bottom. Depending on the withdrawal of material from the bottom opening, an elliptical zone of motion has been observed. The deflection of the originally horizontal thin layers indicates the active zone, that is, the zone with gravity motion of the material. Since the motion is

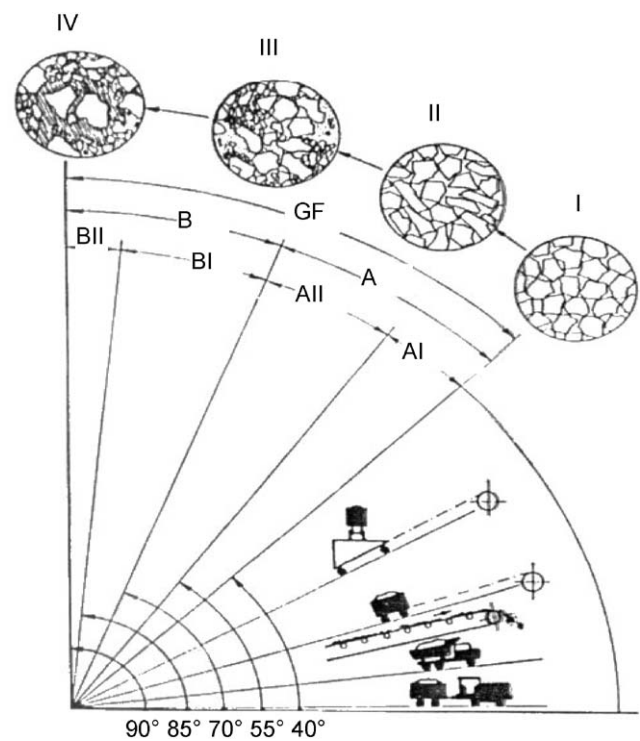


Fig. 5. Four basic types I through IV of coarse material and their mobility as a function of inclination of chute or orepasses (after Ref. [18]).

caused by gravity, the axis of the active zone is stationary. The zone that is not affected by the motion is called the passive zone. As can be clearly seen in Fig. 7b, an ellipsoidal motion zone can be depicted by outlining the active zone. Normally, this ellipsoid consists of the horizontal and vertical regions of a non-symmetrical object, in other words, it is not an ellipse but it is an ellipsoidal cycle and its geometry can be expressed by eccentricity [20,21]

$$\varepsilon = 1/a \left(\sqrt{a^2 - b^2} \right), \quad (1)$$

where, a is the semi-major axis of ellipsoid and b the semi-minor axis of ellipsoid.

3.2. Specific application of sublevel caving to thick-coal seams

For a vertical sublevel front, the sublevel drift forms a vertical opening, located in the plane of the sublevel front. Therefore, on a vertical section, the geometry of sublevel caving is similar to a bin with discharge

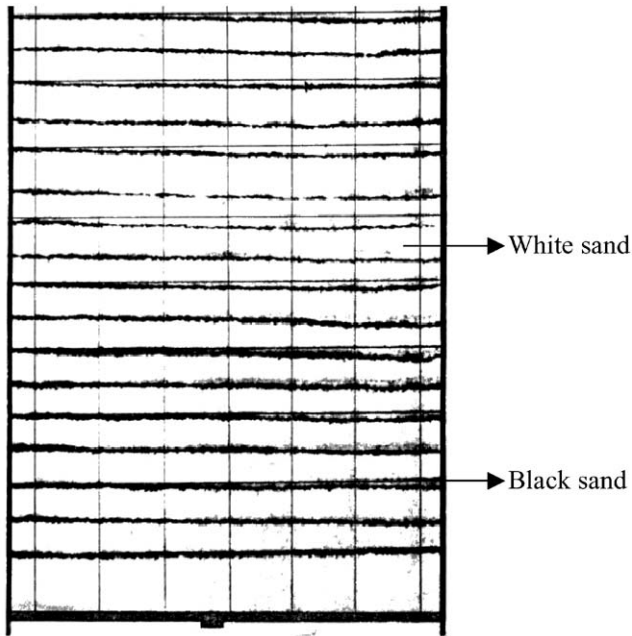


Fig. 6. Simple model of gravity (after Ref. [18]).

openings located at a level above the bottom. The gravity flow zone is cut off by the vertical bin wall but is otherwise unchanged. This means that the vertical wall cuts off the ellipsoid of extraction and loosening as shown in Fig. 8; the axis of gravity flow in this section deviates from vertical by a certain angle Δ . This angle increases as the friction along the vertical wall increases. Neglecting this deviation, one can assume that the vertical wall with discharge opening cuts off half of the ellipsoid of extraction and loosening. Naturally, when this half of the ellipsoid is inscribed in a prism, then its volume is 50% of this prism. Therefore, in sublevel caving, if half of the extraction ellipsoid is inscribed in the body of coal, then a maximum of 50% of coal volume can be extracted without dilution.

In sublevel caving applied at a thick-coal seam, the opening dimensions used for top-coal drawing are limited to the size of the shield window. In order to maintain an efficient flow of the top coal without dilution, dimensions of shield windows should be as low as possible, whereas they should be adequately large enough for the proper flow of top coal. Shield with windows of 80 cm \times 150 cm dimensions are used in the Omerler Underground Mine.

4. Modeling procedure in general

Modeling was carried out with FLAC^{3D} which is used for stress and deformation analyses around surface and underground structures opened in both soil and rock. This software is based on the finite difference numerical method with the Lagrangian calculation method. The

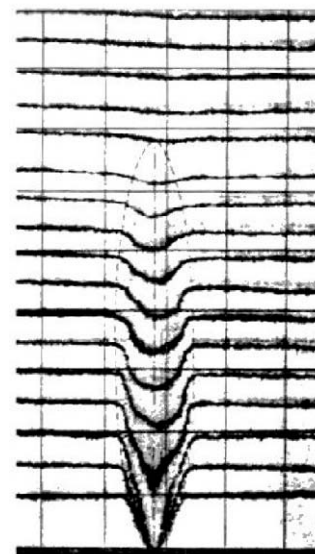
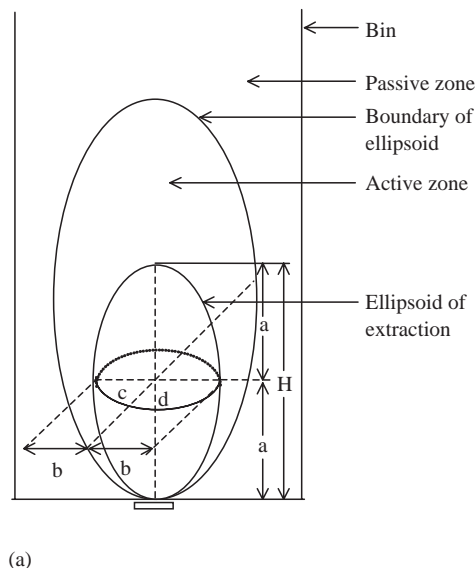


Fig. 7. Successive phase of material extraction from model (after Ref. [18]).

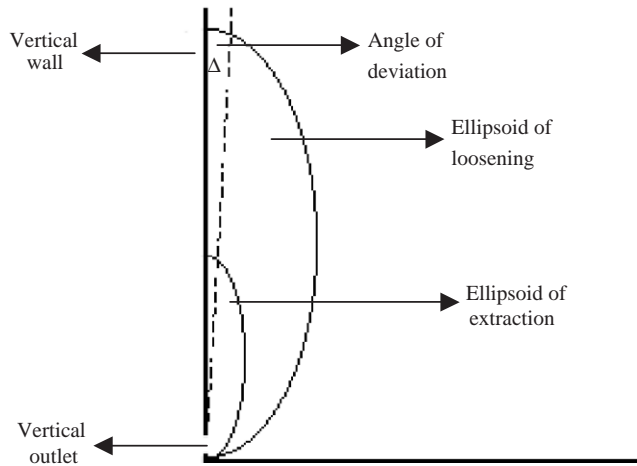


Fig. 8. Schema of ellipsoid of extraction and loosening when material is extracted through vertical outlet in sublevel caving.

Finite Difference method can be better applied to modeling of stress distribution around underground mining excavations in comparison to other numerical techniques. FLAC^{3D} is a commercially available software that is capable of modeling in 3D.

Modeling of longwall with top-coal caving is performed in five steps. Steps identified as A, B, C, D and E are described as follows:

- A. Determination of boundaries and material properties.
- B. Formation of the model geometry and meshing.
Determination of the model behavior.
- C. Determination of the boundary and initial conditions.
Initial running of the program and monitoring of the model response.
- D. Re-evaluation of the model and necessary modifications.
- E. Obtaining of results.

Model geometry and meshing refer to physical conditions of the district to be modeled. Model behavior is the response of a model under a certain loading condition. By means of boundary and initial conditions, physical limits of the model and original conditions are explained. Gate roadways, the face and other structures were later created in the form of modifications. The modeling process is presented in Fig. 9 in a flowsheet form [22].

4.1. Model geometry and meshing

4.1.1. Model for stress distribution around longwall face

Steps of a true scale 3D modeling of the M3 longwall panel with FLAC^{3D} are given as follows:

1. Face length was 90 m at the M3 longwall panel. Therefore, face length was taken as 90 m on the +x coordinate axis in the model.

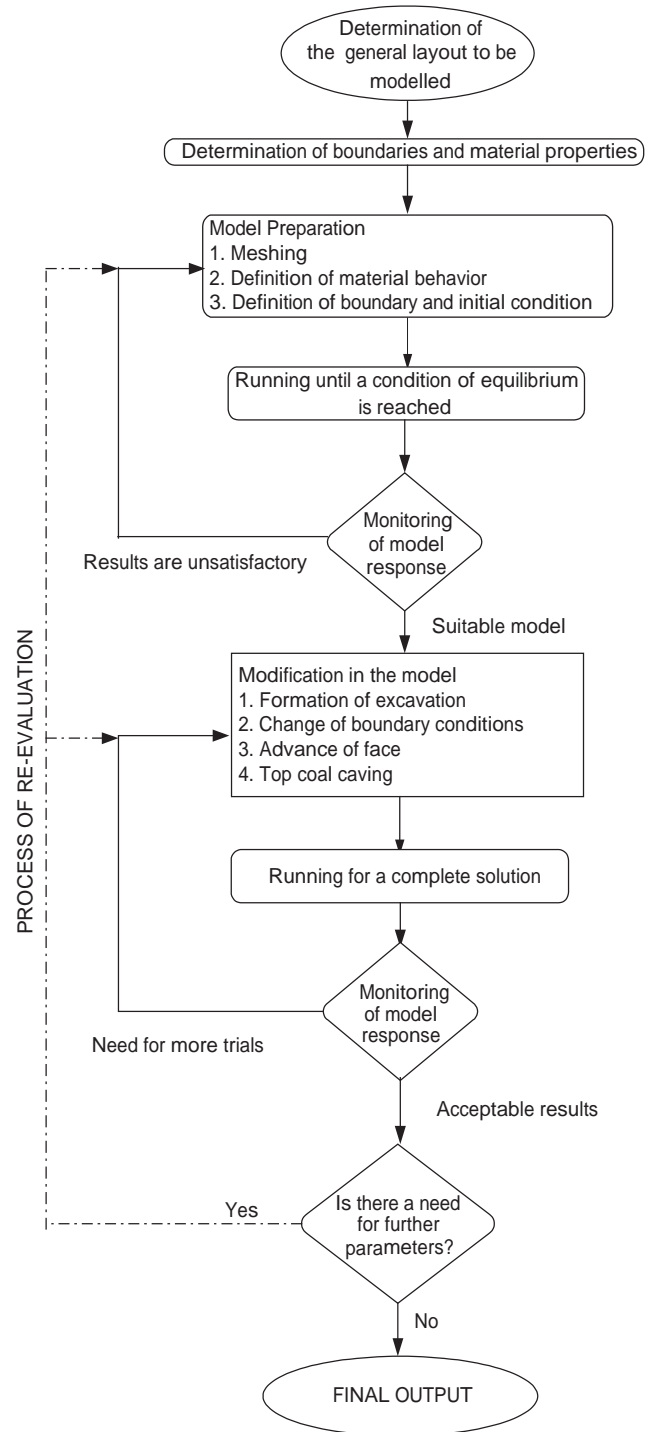


Fig. 9. A general flowsheet of modeling process (after Refs. [7,8,22]).

2. The actual panel length was 450 m. However, due to computer running time and capacity restrictions, the panel length was taken as 250 m on the +y coordinate axis in the model.
3. In accordance with the actual depth below the surface, this value was taken as 240 m on the -z coordinate axis in the model.

4. There was a mined-out panel called M2 separated by a 16 m wide rib pillar. Both the rib pillar and mined-out area were included in the model.
5. In order to obtain more precise stress distribution results, a smaller mesh size was selected at regions in the vicinity of the production area.
6. Quantities of coal cut from the face and caved behind the face were divided into 3 and 5 meshes, respectively.
7. Cubic and prismatic (brick) elements were used for model construction. The model was composed of 16,524 elements and 18,648 grid points as shown in Fig. 10.

4.1.2. Model for top-coal caving

Steps of the 3D modeling of the M3 longwall face and top-coal caving are given as follows:

1. In order to obtain proper results from models formed to analyze caving of top coal, only a small part of the face was modeled. This consisted of the area of two shields located at the face center. Hence, application of a closer meshing in this region facilitated the effective modeling of stresses and displacements.
2. Only the area affected by flowing was constructed.
3. Soft claystone and a 5 m section of roof claystone above the coal were added to the model.
4. In order to properly observe the flowing of top-coal caving, mesh size on the model was formed very closely in three main directions (x , y , z). The model was composed of 42,000 elements and 45,756 grid points, as shown in Fig. 11.

4.2. Assessment of material properties and rock mass strength

It is crucial to properly assess material properties in order to obtain acceptable results in modeling with FLAC^{3D}. Therefore, physical and mechanical properties of each geological unit must be properly determined. In general, intact rock properties are determined by means of laboratory testing. However, there is an important difference between rock material and rock mass characteristics. It is compulsory to determine representative physical and mechanical properties of the rock mass instead of intact rock material. Data regarding the physical and mechanical properties of surrounding rock are given in Table 1. These were obtained by laboratory tests carried out on core samples obtained from exploration drilling and rock blocks taken directly from the mine. Therefore, the data presented in Table 1 are representative only of rock material. It is a rather difficult task to determine rock mass strength characteristics. Therefore, it is a common practice to derive rock

mass strength from rock material properties by using various failure criteria. In this study, rock material properties were converted into rock mass data by using empirical relations widely used in the literature, i.e., Hoek and Brown [23] failure criterion, Bieniawski's [24,25] RMR classification system, and Geological Strength Index (GSI) [26–28]. Physical and mechanical properties of the rock mass used for modeling are presented in Table 2 [3,11,12].

4.2.1. Determination of goaf material properties

Modeling of the caved area is another important step that affects the accuracy of the obtained results. It is a well-known fact that it is a rather difficult task to model goaf material in numerical analyses. Since goaf is mainly made of broken rock pieces, its deformational properties are rather complex due to an ongoing consolidation process with an increase in the amount of load. Xie et al. [29] suggested the following formula for determination of the modulus of elasticity of goaf material with respect to time:

$$E = 15 + 175(1 - e^{-125t}) \text{ MPa}, \quad (2)$$

where t is the time in seconds.

Kose and Cebi [30] suggested a wide interval such as 15–3500 MPa for the modulus of elasticity value for goaf material, whereas Yavuz and Fowell [31] suggested a Poisson's ratio of 0.495 for goaf material for the Tuncbilek Region. These values were used for the characterization of goaf material throughout the analyses.

5. Numerical modeling

5.1. Stress distribution around the longwall face

The model that was made of only solid rock mass not including any openings inside, was solved until a state of equilibrium was reached. After this stage, the model was ready for inclusions of underground mine structures such as roadways and the longwall panel. At first, the main gate and tailgate of the M3 panel were formed in the model with their actual dimensions of 4 m in width and 3 m in height. The location of the main gate and tailgate, together with the rib pillar between the M2 old working panel and the M3 panel and the face can be seen in Fig. 10. In the mine, main gate and tailgate were supported by means of rigid steel arches. However, it was not possible to add such a support type in the model prepared by using FLAC^{3D}. Therefore, it was found convenient to represent supporting in the form of a thin layer of shotcrete as a structural shell element. After the formation of the main gate and tailgate, the longwall face was formed. Actual shield supports for the face were modeled in the form of a structural shell elements

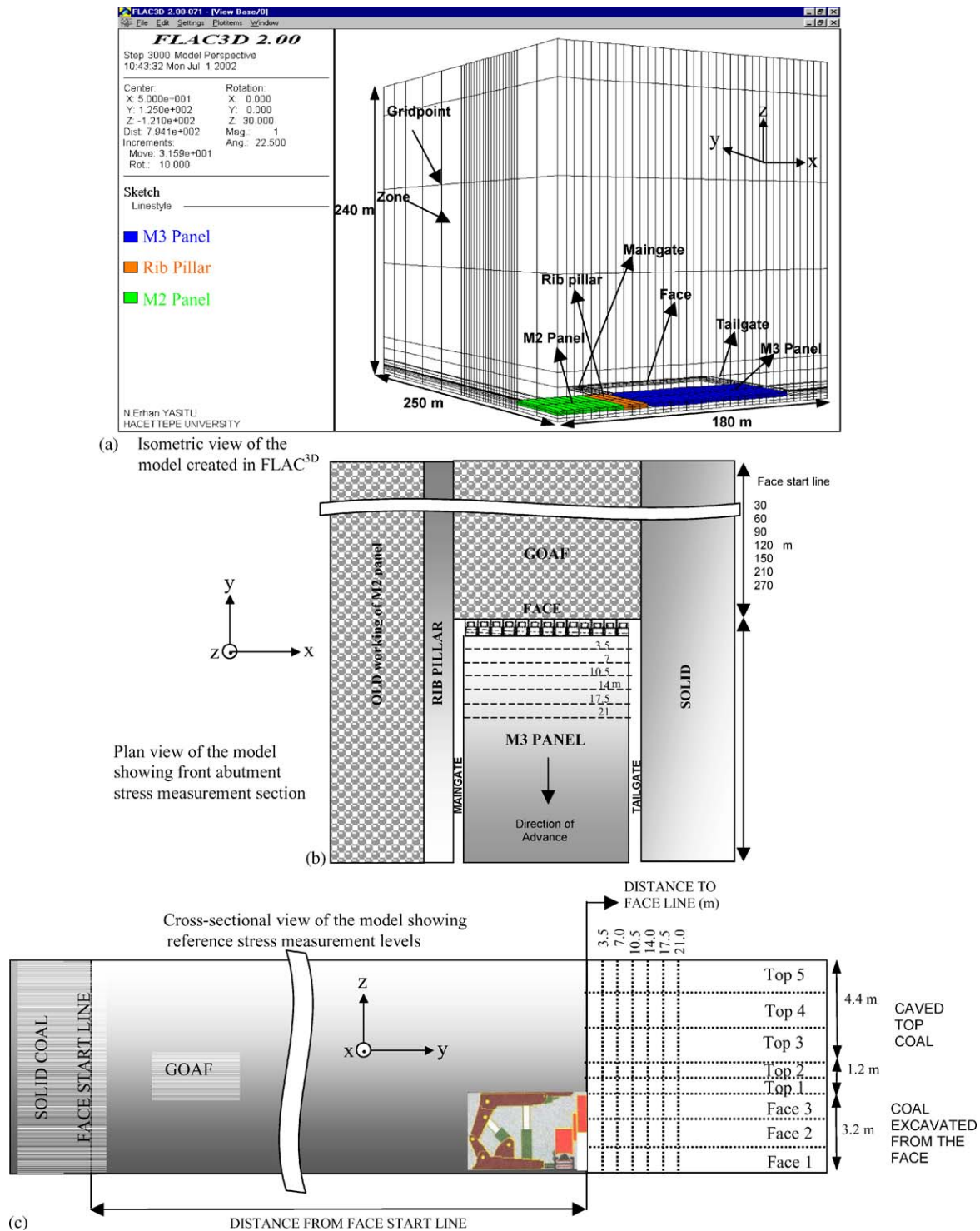


Fig. 10. Details of model geometry of Omerler Underground Mine.

as in gate roadways. Face dimensions were 4 m in height and 3.2 m in width.

5.1.1. Presentation of modeling results

As a result of modeling study depending on face advance, stress and displacement distributions were

found for various conditions. Horizontal stress distribution on the x - and y -axes and vertical stress distribution on the z -axis are presented in Fig. 12 after a face advance of 30 m from the face start line. Fig. 13 presents the distribution of vertical stresses in front of the face at various distances toward the direction of advance from

the face line, such as 3.5, 7, 10.5, 14, 17.5 and 21 m at eight different levels (see Fig. 10) of the coal seam at every 5 m starting from the main gate and proceeding toward the tailgate.

In order to obtain stress distribution in a categorized form, the 8.8 m thick-coal seam was divided into three levels at the face and five levels in the top coal (see Fig. 10).

Horizontal stresses were found to be maximum at 7 m in front of the face in the order of 4.67 MPa in the x -

direction and 4.10 MPa in the y -direction. Maximum vertical stress at the same region was found to be 11.80 MPa. The results revealed that z -, x - and y -directions corresponded to maximum, intermediate and minimum principal stress directions, respectively.

In order to simulate the change in the characteristics of stress distribution around the face, a progressive modeling has been carried out depending on face advance. Therefore, the model was progressively modified after each run as the face was advanced 60, 90, 120 and 150 m away from the face start line. However, in this study, a comprehensive interpretation of these modeling results has not been given. Hence, only the change in vertical stress distribution around the longwall face depending on face advance has been briefly presented.

Stress distribution around longwall faces has been found by various researchers depending on the results of in situ measurements [32–34]. As can be seen in Fig. 14, vertical stress increases in front of the face and gradually decreases to a value equal to field stress at a distance about 0.12 times depth below surface in front of the face. Following the eventual failure of the coal seam in the maximum front abutment region, the maximum vertical stress zone would tend to shift approximately 2 or 3 m away ahead of the face. On the other hand, vertical stress drastically drops to zero at the coal seam roof contact, and then a gradual build-up of vertical stress is observed in the goaf region behind the face, depending on the rate of compaction.

Vertical stress distributions obtained from the model after 30, 60, 90, 120 and 150 m of face advance from the start line are presented in Fig. 15. The magnitude of field stress was calculated as 5.75 MPa and presented with a dashed line in Fig. 15. A comparison of Figs. 14 and 15 clearly indicates that characteristics of the stress distribution obtained by means of numerical modeling

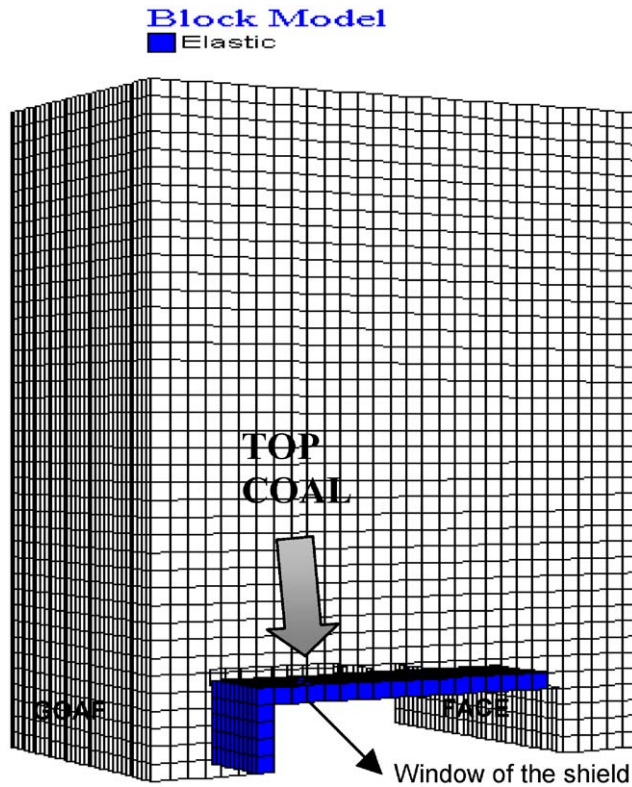


Fig. 11. Top-coal-flowing model constructed in FLAC^{3D}.

Table 2

The input parameters regarding rock mass used in numerical modeling (After Ref. [7,17])

Rock definition	Calcareous marl	Marl	Roof claystone	Soft claystone	Coal	Floor claystone
Density (d) (MN/m ³)	0.023	0.022	0.025	0.023	0.014	0.027
Internal friction angle (ϕ) (deg.)	27.5	24.8	18.8	14.0	21.8	18.4
Cohesion (c) (MPa)	1.3	0.65	0.41	0.167	0.517	0.715
Modulus of elasticity (E) (MPa)	5404	4012	1921	746	1907	2315
Tensile strength (MPa)	0.096	0.074	0.031	0.006	0.017	0.035
Poisson's ratio (ν)	0.25	0.25	0.28	0.25	0.25	0.31
Bulk modulus ^a (K) (MPa)	3603	2675	1281	497	1271	1543
Shear modulus ^b (G) (MPa)	2162	1605	750	298	762	884
Uniaxial compressive strength (MPa)	1.80	1.849	1.131	0.428	1.294	1.981
m_b	1.174	0.838	0.370	0.176	0.563	0.343
S	0.0039	0.0039	0.0008	0.0001	0.0006	0.0005
a	0.506	0.506	0.511	0.522	0.511	0.511

^a $K = E/3(1 - 2\nu)$.

^b $G = E/2(1 + \nu)$.

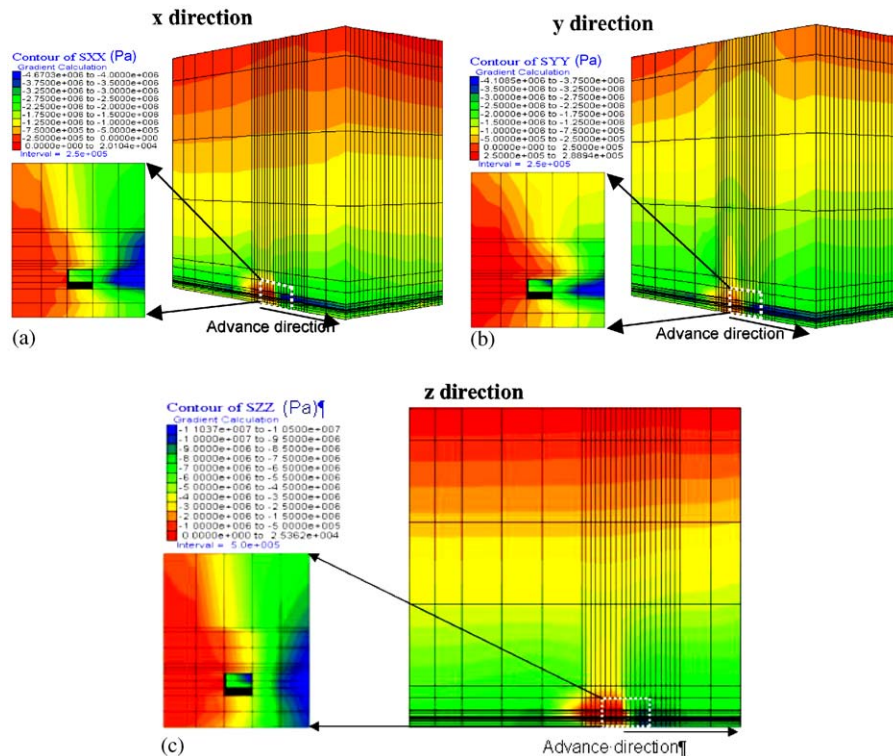


Fig. 12. Distribution of horizontal (x- and y-direction) and vertical (z-direction) stresses around longwall panel.

are in good agreement with the results of actual measurements.

As shown in Fig. 15, the front abutment pressure increases until a distance of 7 m from the face line, reaching to a maximum stress level of 14.4 MPa. After reaching the highest value, the front abutment pressure decreases gradually toward the initial field stress value of 5.75 MPa at a distance of approximately 70 m away from the face. As can be seen in Fig. 15, the vertical front abutment stress at greater than 70 m ahead of the face was about 7–8 MPa whereas the field stress level was 5.75 MPa. This difference was due to the effect of the main gate and tailgate on the solid coal in front of the face, since the M3 panel was produced by means of the retreat longwall method with a relatively short face length of 90 m. The abutment stress formed at a distance of 7 m in front of the face was found to increase 2.6-fold according to initial field stress. Stress in the goaf behind the face decreases to around 0.1 MPa levels and tends to increase at the start line of the face in a manner similar to front abutment stresses. At the face start line of the panel, rear abutment stresses reach the highest level at 2–3 m inside the solid coal and decrease gradually to the field stress level at about 60 m inside the solid coal.

5.2. Top-coal caving through the window of a shield

Top-coal caving through the window of a shield was modeled. Figs. 16a and b present the modeling results of

top-coal caving for a single shield along AA' and BB' cross-sections perpendicular and parallel to the face, respectively. Each color (or tone) corresponds to a certain amount of vertical displacement in the figures. Displacement values are given in meters such as 1.95e00.1 value, meaning that the region of this color corresponds to a vertical displacement amount of 195 mm. The active zone and the boundary of the ellipsoid of motion are shown in Figs. 16a and b. Similar to the case shown in Fig. 16a, the amount of vertical displacement is the highest at the shield window, decreasing considerably away from this region. The region of high vertical displacement is called the ellipsoid of motion and the region outside the ellipsoid of motion where lower displacements are observed is called the active zone. As the name implies, the region that is not affected is called the passive zone. As coal is drawn through the window of a shield, the top coal in the active zone enters the ellipsoid of motion until all of the top coal is produced.

Failure mechanism of top coal during drawing is presented in Fig. 17. Explanations of terms given in the legend are as follows:

- none: no-failure zone,
- shear-n: the region failed under shear loading and failure process is still in progress,
- shear-p: the region failed under shear loading and failure process is ceased due to lowered amount of shear forces,

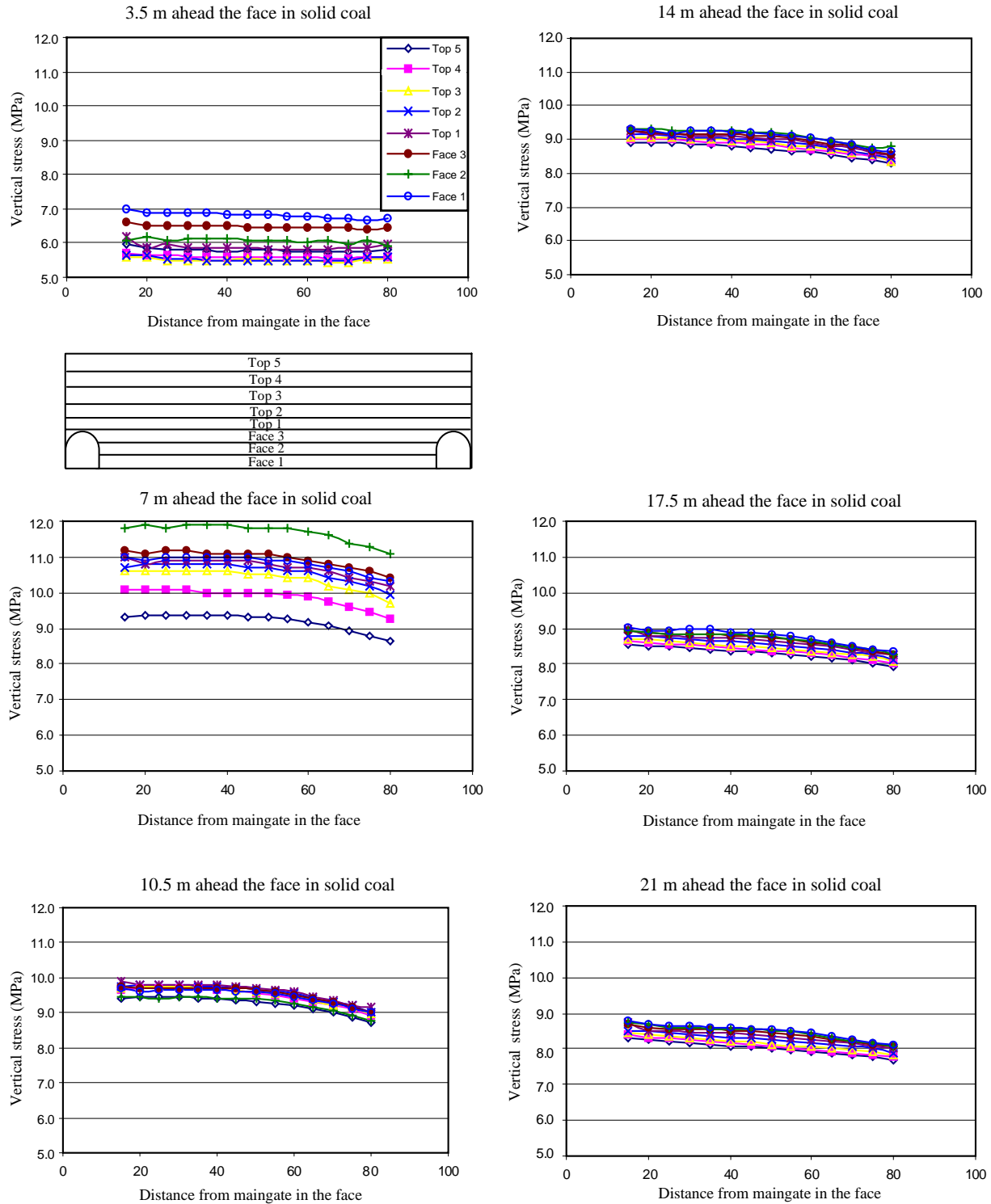


Fig. 13. Vertical stress distribution around the face at various intervals perpendicular to face.

tension-n: the region failed under tensile loading and failure process is still in progress,
 tension-p: the region failed under tensile loading and failure process is ceased due to lowered amount of tensile forces.

Results obtained from modeling indicate that a 1.5 m thick layer of coal just above the shield supports is well fractured (shear-n). However, due to the results of lowered shear loads (shear-p), the coal above 1.5 m is not fractured completely. Characteristics of failure

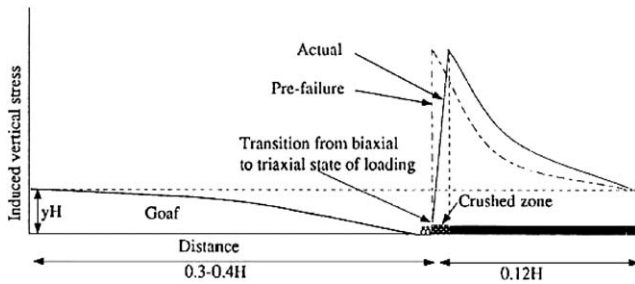


Fig. 14. A model of stress redistribution around a coal mining face (after Refs. [32–34]).

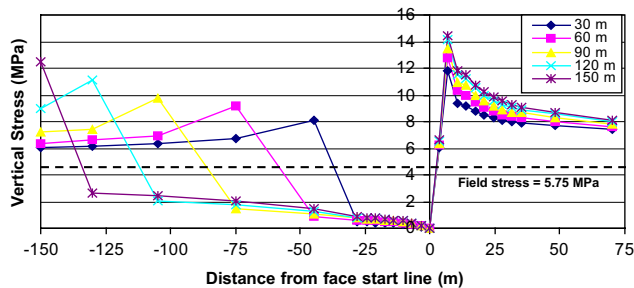


Fig. 15. Vertical stresses around the face and goaf forming with face advance.

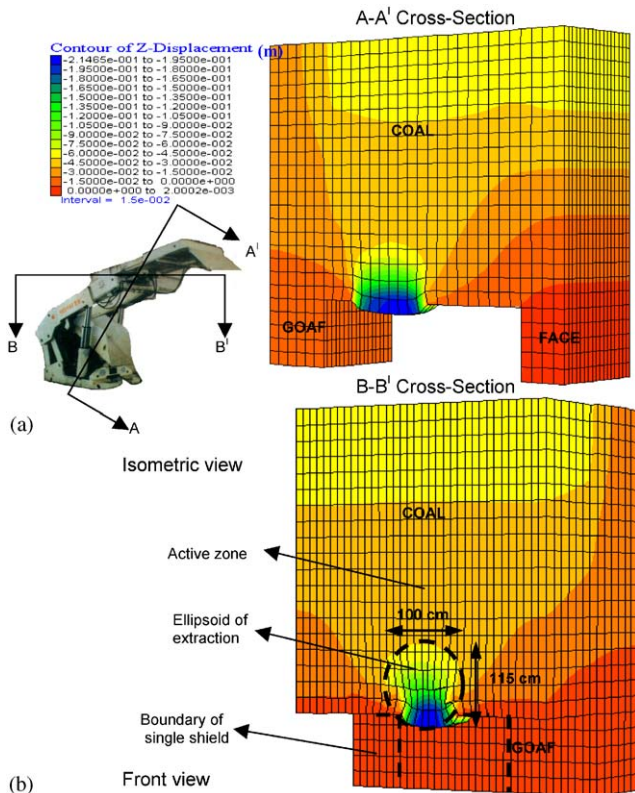


Fig. 16. Modeling of top-coal caving.

phenomenon obtained from the modeling study show that there would be no problem during caving and drawing of the first 1.5 m from the shield top as a result

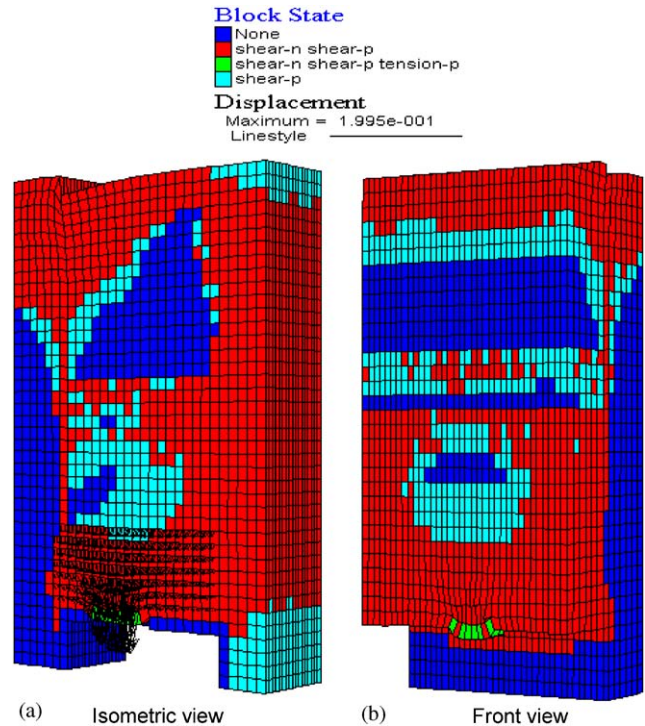


Fig. 17. Vertical state of failure in top coal during caving.

of high vertical and shear stresses (shear-n). However, above this well-fractured section the coal does not fail completely. Failure is observed occasionally for some time and stops as a result of decreasing shear loads (shear-p). This means that coal would be broken into larger pieces starting from 1.5 m above the face roof. As a result, larger pieces would block the shield window, and there would be serious problems such as prevention of continuous flow of top coal, interruption of production at the face and a decline in the quality of coal produced. This phenomenon is well observed in the mine. In the mine, there was no problem at the beginning of coal drawing. Later, as a result of increased block size in the drawn coal, possibility of blockage increased. Whenever such a problem was faced in the mine, the block obstructing the window was blasted and then drawing operation resumed.

In Fig. 17, there seems to be no deformation (none) behind the face. The reason for this situation is that the material behind the face in the goaf is defined as failed material at the beginning of modeling. Since stress build-up in the failed goaf cannot be high enough, no post failure is observed in this region as expected.

Top-coal caving through windows of shields was performed in one shift at the Omerler Underground Mine. During top-coal caving, adequate fastidiousness was not applied and orders of top coal flowing through windows of shields were not observed by workers. For these reasons, shield windows have also not been opened

in a proper order. When top-coal caving through one window was finished, the adjacent window was opened. Therefore mixing of waste rock in the coal was increased, leading to an increase in dilution and decrease in productivity and production rate. In order to decrease dilution and increase the rate of extraction, top coal had to be fractured as uniformly as possible and windows of shields had to be sequentially opened.

5.3. Suggested method for top-coal caving

The upper part of the thickcoal seam at the Omerler Region is stronger than the lower part. As a consequence, formations of large blocks were observed during caving of the upper part of coal seam caving in the mine. This situation was verified by means of numerical modeling results. As numerical modeling results have indicated, the upper part of the top coal was not uniformly fractured and, consequently, during flowing of top coal, shield windows were usually obstructed by large blocks. In the case of obstruction of the shield windows in the mine, large blocks were broken into small pieces either by drilling and blasting or by moving the shield up and down. The length of the blastholes was between 3–6 m. Drilling and blasting seemed to temporarily solve obstruction problems; however, large blocks are fractured into irregular shapes with a wide range of particle-size distribution by blasting. As can be seen in Fig. 5, the angle of flowing coal having a wide range of particle-size distribution is higher than the angle of flowing coal that has an approximately uniform particle-size distribution. During the flowing process of top coal through the window of a shield, coal having a wide range of particle-size distribution results in both mixing the coal to the goaf and also dilution of surrounding rock into the coal produced. Being a time consuming operation, blasting of large blocks would not enhance flowing characteristics of top coal; to the

contrary, productivity is significantly decreased. In order to maintain a high rate of advance with an increased rate of recovery, formation of large blocks should be prevented as often as possible. This can be accomplished by means of pre-fracturing or pre-cracking of top coal prior to the caving operation. In order to minimize the time-consuming and tedious operation of the large block blasting method and to increase productivity and daily advance rate and to decrease dilution, large blocks have to be fractured into small pieces by the application of pre-fracture blasting carried out at the boundary of the top coal; consequently, providing a more uniform particle-size distribution. The proposed method of blasting must be carried out at the boundary of the top coal, not at the face. The objective of this operation is not to fracture the top coal completely, but to provide a more uniform size distribution in the coal as a result of pre-fracture blasting (Fig. 18). It is suggested to open inclines from main gate and tailgate to the upper boundary of the top coal at a distance of 20–25 m in front of the face. The blasting should be carried out only for forming cracks in the top coal to enhance caving characteristics of the top coal located at 3–3.5 m above the face. In other words, the objective of blasting is not to fracture top coal completely but to form cracks that would help the formation of a regular particle-size distribution during caving. In this manner, the possibility of existence of large blocks in the top coal will be decreased, leading to formation of top coal having a particular size that can easily flow through the windows of a shield. The quality of coal produced behind the face will be improved and the extraction ratio of reserve will also be increased due to less dilution. Besides, blasting carried out in the top coal in front of the face would be carried out independently from operations carried out at the face. Thus time required for blasting will be eliminated and consequently productivity would also be increased.

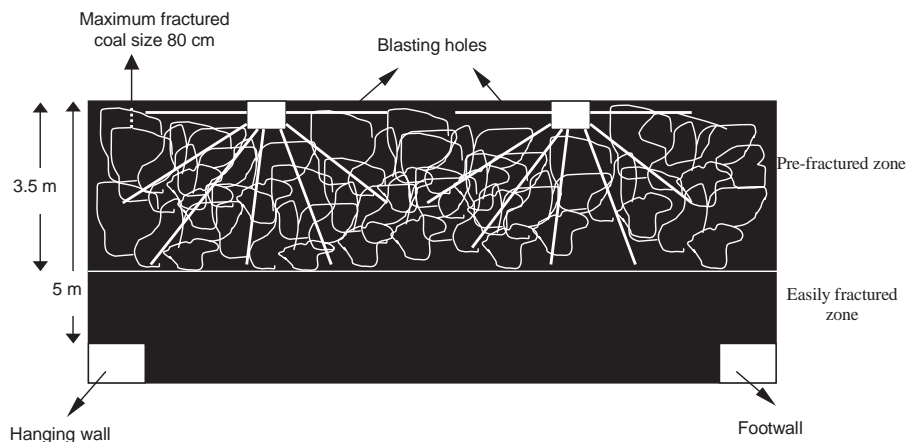


Fig. 18. Suggested blasting design.

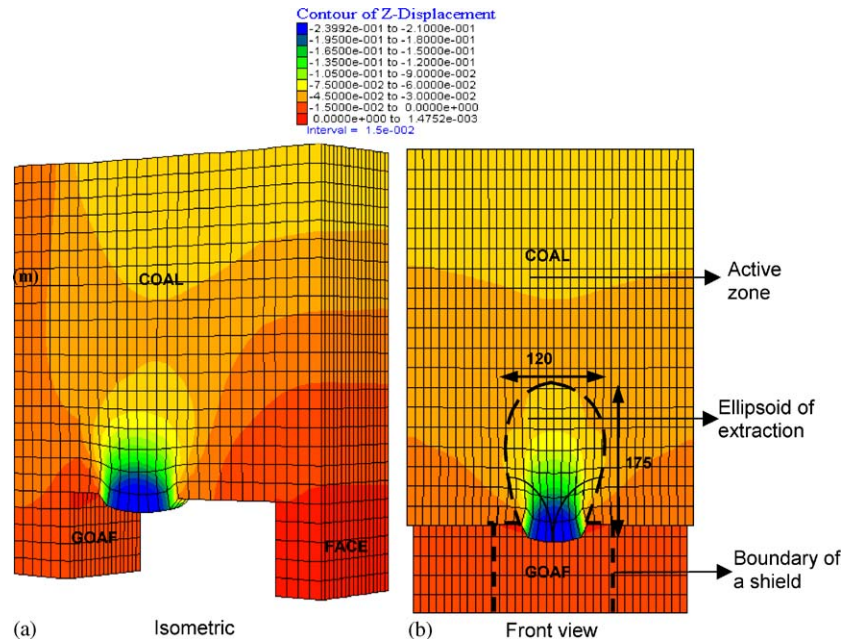


Fig. 19. Modeling of top-coal caving after pre-fracture blasting.

5.4. Modeling of top-coal caving after pre-fracture blasting

Caving of top coal through the window of a single shield after blasting has been modeled and Fig. 19 presents modeling results of top-coal caving. The boundary of a shield, ellipsoid of extraction and active zone are shown in Fig. 19b. As can be seen in Fig. 19, displacement is the highest at the window discharge. In other words, the flowing rate of top coal is higher at this region, but outside this region the displacements are low.

The modeling results revealed that during top coal flowing through the window of a shield, coal above the shield was well fractured (shear-n) due to decrease in the mechanical properties of coal after pre-fracture blasting (Fig. 20). This means that the coal was fractured as uniformly as possible and formation of large blocks was not allowed. Hence, all parts of the top coal can be continuously drawn through the window of a shield; dilution will be reduced and problems encountered due to obstruction of windows would be reduced or eliminated.

5.5. Evaluation of modeling results of longwall with top-coal-caving method

After two modeling studies for longwall with top-coal-caving method, the results given below were found;

- The width and height of ellipsoid of extraction are 100 and 115 cm, for the flowing of top coal through the window of a single shield.

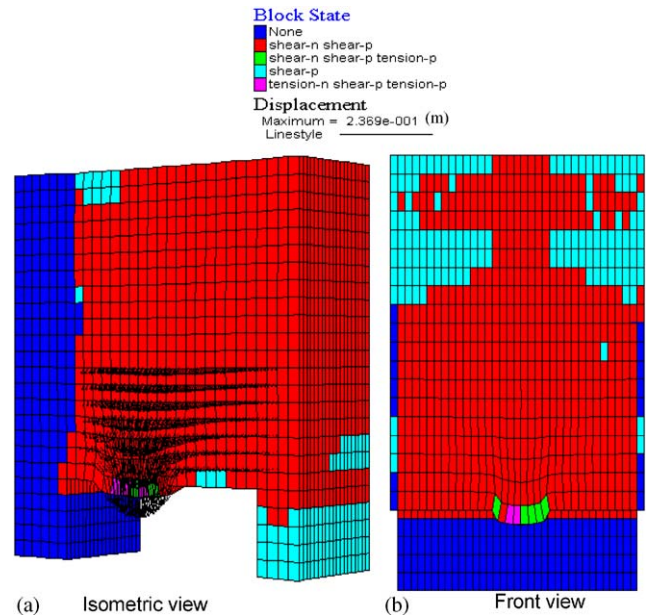


Fig. 20. State of failure in top coal during caving after pre-fracture blasting.

- The width and height of ellipsoid of extraction are 120 and 175 cm, for the flowing of top coal through the window of a single shield after pre-fracture blasting.

As can be seen in Fig. 21, although the width of the ellipsoid of extraction has not been changed significantly, the height of the ellipsoid of extraction was increased by means of pre-fracture blasting. The reason for this is the eccentricity of coal (Eq. (1)). If eccentricity

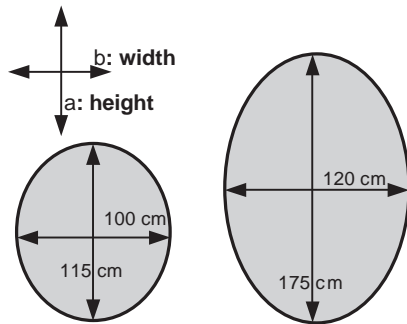


Fig. 21. The width and height of ellipsoid of extraction before and after pre-fracture blasting.

is high, the ellipsoid of extraction will become narrow; if the eccentricity is low, the ellipsoid of extraction becomes wider.

If ellipsoids of extraction obtained from modeling results are compared with each other, it can be seen that the height/width ratio (h/w) of ellipsoids of extraction is low due to a wide range of particle-size distribution of top coal before pre-fracture blasting. However, h/w ratio is higher after pre-fracture blasting because of more uniform particle-size distribution of coal. These results reveal that the amount of flowing material through the shield windows will be high for a given unit time.

6. Suggested top-coal-caving order

As stated earlier, formation of large blocks having the potential to obstruct shield windows should be prevented as much as possible, and top coal should be fractured as uniformly as possible. Production of top coal by means of drawing through windows located at the canopy of shields should be performed in a predetermined sequence, as shown in Fig. 22. Although there were 60 shields at the M3 longwall face, only ten of them are shown in Fig. 22 for the sake of simplicity.

After pre-fracture blasting, the top coal flowing through shield windows can be carried out in three ways as follows:

- i. Top coal flowing through windows starting either from face head to face end or from face end to face head.
- ii. Top coal flowing through windows starting either from face center to face head or face end.
- iii. Top coal flowing through windows starting either from face head or face end to face center.

Top coal having as uniform particle-size distribution as possible after the pre-fracture blasting operation has to be drawn as fast as possible with great care. It is considered that there would not be any major problem

during application of methods given in Fig. 22. In order to flow top coal rapidly, two crews have to be organized. Simultaneously the first team can start flowing top coal from the face head, and the second team can start from the face end; or both teams can start flowing from the face center to face head and face end by drawing half of the top coal while in advance and the other half while returning to the starting point (Fig. 22). Flowing of top coal through either a single or multiple shield windows does not significantly affect dilution.

7. Conclusions

In this study, 3D modeling of a longwall with the top-coal-caving method applied at the Omerler Underground Mine was carried out by FLAC^{3D}. For realistic modeling, material properties were derived for the rock mass from laboratory data by using Hoek–Brown failure criterion, the RMR and GSI systems together with empirical equations. Results of this modeling study have revealed that the maximum vertical abutment stresses (14.4 MPa) were found at a distance of 7 m in front of the face; a later of top coal 1.5 m above the shield is well fractured at a particular size that can flow easily through shield windows. However, the coal above this fractured zone either could not be fractured at all or fractured in the form of large blocks. Results of numerical modeling coincided with the in situ observations carried out in the mine. In the M3 panel, when the windows of shields were obstructed with large blocks, these were fractured by means of drilling and blasting. At first glance, this operation seems to solve the problem. However, blasting leads to formation of a wide range particle-size distribution in the top coal. Hence, a portion of the top coal is lost in the goaf and part of the roof claystone is mixed with the coal produced, eventually causing dilution.

Pre-fracture blasting, which was designed to fracture top coal further above 3.5 m from the shield top is aimed not at fracturing the top coal completely, but at forming a more or less uniform size distribution. After application of pre-fracture blasting, top-coal caving through windows of shields can be carried out effectively; consequently, dilution can be reduced with increased productivity.

As a final conclusion derived from numerical modeling results and in situ observations, despite high investment cost, pre-fracture blasting has to be performed above the face at the coal boundary and uniform size distribution has to be obtained in the top coal prior to production. It is determined that top coal has to be flowed in the form of sequential slices. These operations will certainly reduce dilution, increase production and face advance rate.

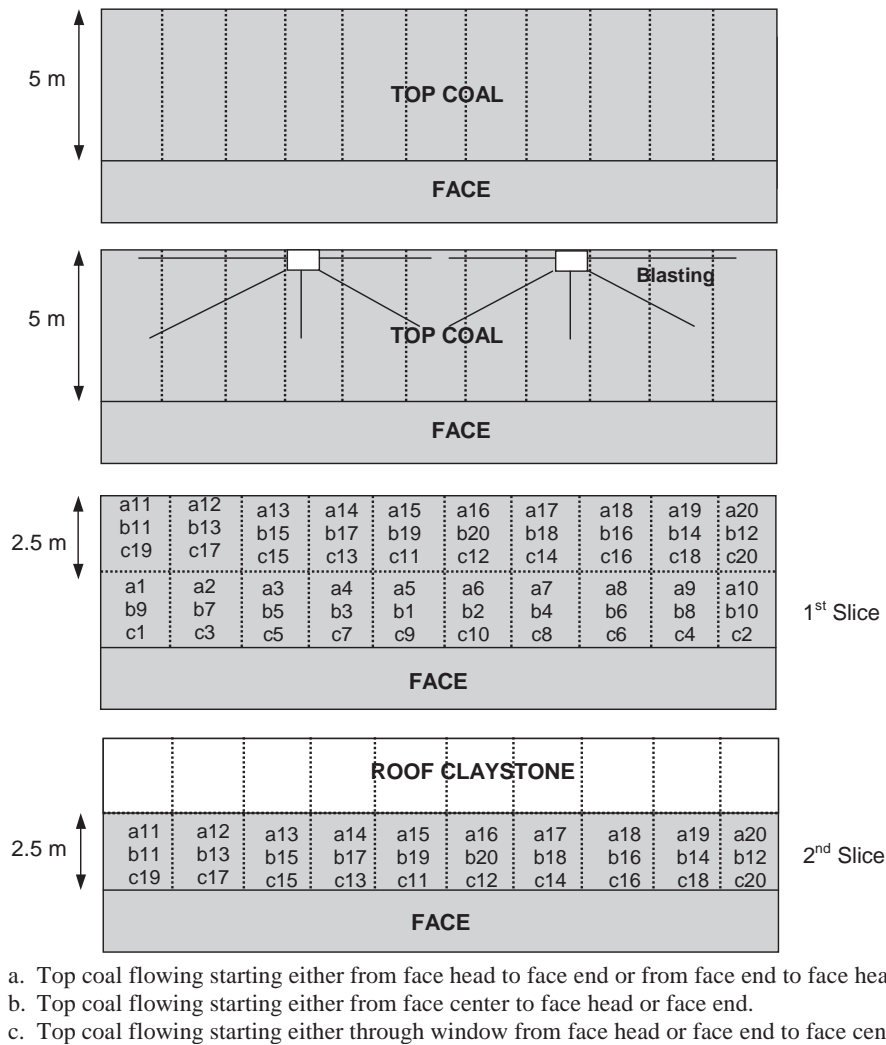


Fig. 22. Designed top-coal-caving order.

Acknowledgements

The results of this paper are based on a research project funded by Hacettepe University, Scientific Researches Unit. The authors are obliged to Dr. F.B. Tasking for providing help during the field trial. Thanks are due to the management of the Turkish Coal Enterprise and Omerler Colliery for their valuable cooperation during fieldwork.

References

- [1] Singh R. Mining methods to overcome geotechnical problems during underground working of thick coal seams-case studies. *Trans Inst Min Metall (Sec A: Min Indus)* 1999;108:A121–31.
- [2] Atkinson T. Thick, steep and irregular coal seam mining. *The Min Eng* 1979;421–41.
- [3] Senkal S, Kose H, Ermisoglu N. A study on coal losses and dilution problems in the mining method applied at GLI Tuncbilek Colliery. *Madencilik, Bull Chamber Min Eng Turkey* 1988;27(4): 5–11 (in Turkish with English abstract).
- [4] Schweitzer R. Thick seam winning methods in French coal mines. *Proceedings of the international symposium on thick seam mining, Dhanbad, India, 1977, paper no. 3.*
- [5] Ahcan R. Mechanization and concentration of thick coal seams mining in SFR Yugoslavia. *Proceedings of the international symposium on thick seam mining, Dhanbad, India, 1977, paper no. 4.*
- [6] Garg PC, Nath PD. Choice of methods for mining thick coal seams in India. *Proceedings of the international symposium on thick seam mining, Dhanbad, India, 1977, paper no. 10.*
- [7] Yasitli NE. Numerical modeling of longwall with top coal caving. M.Sc. thesis, Hacettepe University, Ankara, 2002. p. 148 (in Turkish).
- [8] Unver B, Yasitli NE. Simulation of sublevel caving method used in thick coal seam by computer. *Hacettepe University Scientific Research Unit, Project no: 00 02 602 008, 2002. p. 148 (in Turkish).*
- [9] Tien J. Longwall caving in thick seams. *Coal Age* 1998;103(4): 52–61.
- [10] Jeremic ML. *Strata mechanics in coal mining*. Rotterdam: A.A. Balkema; 1985. p. 556.
- [11] Jha SN, Karmakar S. Thick seam mining-some experience and exaltation. In: Singh TN, Dhar BB editors. *Proceedings of the international symposium on thick seam mining, India, Dhanbad: Central Mining Research Station; 1992. p. 191–202.*

- [12] Singh TN, Kushwaha A, Singh R, Singh R. Strata behaviour during slicing of thick seam at East Katras Colliery. In: Singh TN, Dhar BB editors. *Proceedings of the international symposium on thick seam mining*. Dhanbad, India: Central Mining Research Station; 1992. p. 237–50.
- [13] Dian C. The state of the art and future of China thick seam mining technology. In: Singh TN, Dhar BB editors. *Proceedings of the international symposium on thick seam mining*. Dhanbad, India: Central Mining Research Station; 1992. p. 171–82.
- [14] Wu J. The movement regularity of the roof coal around a longwall with caving and its coal recovery. *Proceedings of the international symposium on fully mechanized mining technology for high output and efficiency*. 1992. p. 307–18.
- [15] Destanoglu N, Taskin FB, Tastepe M, Ogretmen S. Application of GLI Tuncbilek–Omerler underground mechanization. Ankara: Kozan Publishing, Ankara; 2000. p. 211. (in Turkish).
- [16] Taskin FB. Optimum dimensioning of pillars between longwall panels in Tuncbilek Mine, PhD thesis, Osmangazi University, Eskisehir, 1999. p. 149 (in Turkish).
- [17] Yasitli NE, Unver B. 3D estimation of stresses around a longwall face by using finite difference method. 18th international mining congress of Turkey, Antalya, 2003. p. 83–8.
- [18] Kvapil R. Sublevel caving. *SME mining engineering handbook*. 1992. p. 1789–814.
- [19] Unver B. A practical approach to strata control and caving mechanism in thick seam mining. 14th mining congress of Turkey, Ankara, 1995. p. 15–22 (in Turkish).
- [20] Kvapil R. The mechanics and design of sublevel caving systems. In: Gertsch RE, Bullock RL editors. *Techniques in underground mining*. SME Inc: Littleton, USA; 1998. p. 621–54.
- [21] Julin P, Kvapil R. Caving methods. In: Hustrulid WA editor. *Underground mining methods handbook*. New York: Society of Mining Engineers of The American; 1982. p. 871–93.
- [22] Itasca. User manual for FLAC^{3D}, version. 2.0. Minnesota: Itasca Consulting Group Inc.; 1997.
- [23] Hoek E, Brown ET. Practical estimates of rock mass strength. *Int J Rock Mech Min Sci* 1997;34(8):1165–86.
- [24] Bieniawski. ZT. Engineering classification of jointed rock masses. *Trans S Afr Inst Civ Eng* 1973;15:335–44.
- [25] Bieniawski. ZT. Engineering rock mass classifications, a complete manual for engineers and geologists in mining, civil and petroleum engineering. New York: Wiley; 1989 251pp.
- [26] Hoek E. Strength of rock and rock masses. *ISRM News J* 1995;2(2):4–16.
- [27] Sonmez H. Investigation on the applicability of the Hoek-Brown criteria to the failure of fissured clays. PhD thesis, Hacettepe University, Ankara, 2001. p. 215 (in Turkish).
- [28] Sonmez H, Ulusay R. Modifications to the Geological Strength Index (GSI) and their applicability to stability of slopes. *Int J Rock Mech Min Sci* 1999;36(6):743–60.
- [29] Xie H, Chen Z, Wang J. Three-dimensional numerical analysis of deformation and failure during top coal caving. *Int J Rock Mech Min Sci* 1999;36(6):651–8.
- [30] Kose H, Cebi Y. Investigation the stresses forming during production of thick coal seam. 6th coal congress of Turkey, Zonguldak, 1988. p. 371–83 (in Turkish with English abstract).
- [31] Yavuz H, Fowell RJ. Softening effect of coal on the design of yield pillars. In: Lyon, France D, Billaux et al, editors. *Proceedings of the 2nd international FLAC conference*. Lisse, A.A. Balkema, 2001. p. 313–20.
- [32] Singh R, Mandal PK, Singh AK, Singh TN. Cable-bolting-based semi-mechanised depillaring of a thick-coal seam. *Int J Rock Mech Min Sci* 2001;38:245–57.
- [33] Sheorey PR. Design of coal pillar arrays and chain pillars. *Comprehensive rock engineering*. vol. 2. Oxford: Pergamon Press; 1993.
- [34] Wilson AH. Pillar stability in longwall mining. In: Chugh YP, Karmis M editors. *State of the art of ground control in longwall mining science*. SME: New York; 1982. p. 85–95.